Toward a marginal Arctic sea ice cover: changes to freezing, melting and dynamics

Rebecca Frew[1], Danny Feltham[1], David Schröder[1], and Adam Bateson[1]

[1]Department of Meteorology, University of Reading

Correspondence: Rebecca Frew (rebecca.frew@reading.ac.uk)

Abstract.

As summer Arctic sea ice extent has retreated, the marginal ice zone (MIZ) has been widening~~and making up an increasing percentage of the summer sea ice~~. The MIZ is defined as the region of the ice cover that is influenced by waves, and for convenience here is defined as the region of the ice cover between sea ice concentrations (~~area fractions) A~~ SIC) of 15 to 80%. The MIZ is projected to become a larger percentage of the summer ice cover, as the Arctic transitions to ice free summers. We compare individual processes of ice volume gain and loss in the ice pack (~~A~~SIC>80%) to those in the MIZ to establish and contrast their relative importance and examine how these processes change as the summer MIZ fraction ~~and amplitude of the seasonal sea ice growth/melt cycle increases over decadal timescales.~~ increases over time. This is the first study (to our knowledge) that separately considers the pack ice and MIZ in this way. We use an atmosphere-forced, physics-rich sea ice-mixed layer model (CICE) that includes a joint prognostic floe size ~~distribution (FSD~~and ice thickness distribution (FSTD) model including brittle fracture and form drag. The model has been compared to ~~FSD~~ floe size distribution observations, satellite observation of sea ice extent and PIOMAS estimates of thickness.

The MIZ fraction of the July sea ice cover, when the MIZ is at its maximum extent, increases by a factor of 2 to 3, from 14% (20%) in the 1980s to 46% (50%) in the 2010s in NCEP (HadGEM2-ES) atmosphere-forced simulations. In a HadGEM2-ES forced projection the July sea ice cover is almost entirely MIZ (93%) in the 2040s. Basal melting accounted for the largest proportion of melt in regions of pack ice and MIZ for all time periods. During the historical period, top melt was the next largest melt term in pack ice, but in the MIZ top melt and lateral melt were comparable. This is due to a relative increase of lateral melting and a relative reduction of top melting by a factor of 2 in the MIZ compared to the pack ice. The volume fluxes due to dynamic processes decreases due to the reduction in ice volume in both the MIZ and pack ice. As ~~the~~ more of the summer ice cover becomes ~~marginal (MIZ)~~MIZ, it melts earlier: in the region that was pack ice in the 1980s and became ~~marginal~~ MIZ in the 2010s, peak melting starts 20~~/~~(12~~days earlier (NCEP/HadGEM2-ES)~~) days earlier. This continues in the projection where melting in the region that becomes MIZ in the 2040s shifts 14 days earlier.

1 Introduction

The marginal ice zone (MIZ) is ~~traditionally~~ defined as the region of the sea ice cover influenced by ocean waves (Dumont et al., 2011; Horvat et al., 2020). Here, however, we have applied the often used and more easily applied definition of the MIZ

as the region covered by 15-80% sea ice concentration ~~(Rolph et al., 2020; Aksenov et al., 2017; Strong and Rigor, 2013)~~(SIC) (Strong and Rigor, 2013; Aksenov et al., 2017; Rolph et al., 2020). The pack ice ~~if~~ is defined as the region where the ~~ice concentration~~ SIC exceeds 80%. The MIZ grows in early summer as the sea ice cover starts to melt and become more fragile. This leads to an increase in fragmentation creating a higher ~~concentration~~ fraction of smaller floes. As the sea ice cover shrinks to its minimum extent~~in~~ , the MIZ contracts too. The MIZ forms a much smaller fraction of the sea ice cover throughout the winter months. As summer Arctic sea ice has retreated over the past 40 years the ~~MIZ~~ fraction of the summer ~~Arctic~~ sea ice cover ~~has been increasing~~ that is MIZ has increased (Rolph et al., 2020). This trend is projected to continue (Strong and Rigor, 2013; Aksenov et al., 2017). In this work we consider how the processes of ice gain and loss in the MIZ and the pack ice differ, and what this may mean for the future Arctic sea ice cover.

~~The sea ice concentration budget~~ The strength of sea ice is strongly dependent on the SIC. For 80% SIC (the upper MIZ boundary), we can estimate (Hibler, 1979) that ice strength is less than 2% of its maximum. In the MIZ internal stresses in the ice play only a small role and sea ice is essentially in free drift. The sea ice in the MIZ behaves distinctly to pack ice as it can be more easily advected. This has implications for those wanting to cross the Arctic: a larger Arctic MIZ would be easier to send ships across.

The larger concentration of smaller floes and lower sea ice concentration in the MIZ has a number of consequences for the sea ice interactions with the ocean and atmosphere. Lateral melting will be enhanced due to the increased perimeter to surface area ratio, creating open water more efficiently than top or basal melt, and potentially fuelling the ice-albedo feedback. The lower the ice concentration, the more the surface ocean is warmed due to the lower albedo of open ocean, further enhancing ice melt and leading to the positive ice-albedo feedback. The increased open water fraction can also mean an increase in wind mixing in the mixed layer and will affect Arctic Ocean spin up (e.g. Martin et al. (2016)). There is a wave-floe size feedback that means the smaller the floes, the larger the impact of the waves, so a positive feedback loop exists that can act to increase the action of waves on the sea ice floes and further increase the concentration of smaller floes. The location and volume of sea ice melt has implications for stratification and so how deeply solar heat is mixed down. More sea ice melt means the mixed layer is shoaled and solar heat is concentrated in the upper water column.

Meanwhile there are other important sea ice processes, such as top melting where it is less clear that we would expect there to be a contrast between the MIZ and the pack ice, for example in the formation of melt ponds. In the Arctic, the snow thickness is generally modest compared to that on Antarctic sea ice, and the location of top melting and the formation of surface melt ponds is primarily driven by atmospheric conditions. Projections suggest that the MIZ will increasingly dominate the Arctic sea ice cover, especially in summer. It seems likely, therefore, that MIZ-focussed processes will play an increasing role in controlling the mass budget of Arctic sea ice.

The SIC budget from observations has been constructed for the Arctic by Holland and Kimura (2016) using AMRS-E satellite observations spanning 2003-2010, comparing the relative roles of thermodynamic and dynamic processes through the seasonal cycle. There is no equivalent for ice thickness and volume using observations yet, but a number of studies have assessed the Arctic sea ice mass budget in climate models (Holland et al., 2010; Keen and Blockley, 2018; Keen et al., 2021). Holland et al. (2010) assessed CMIP3 models and found a large amount of variation between the relative importance of

processes as Arctic sea ice declined. They also found that the initial sea ice state was important in determining projected changes to the sea ice cover, with thicker initial ice resulting in more sea ice volume change.

Following the framework set out by the Sea-Ice Model Intercomparison Project (SIMIP) in Notz et al. (2016) for comparing the energy, mass and freshwater budgets, Keen et al. (2021) compared the sea ice mass balance in CMIP6 models over the 21st century. Although Keen et al. (2021) also found significant differences in the changes to the mass budget component size and timing between the models, they found that when the sea ice state is taken into account the models behave in a similar fashion to warming, with melting happening earlier in the summer and growth reducing in autumn and increasing in winter over the coming decades.

In this study we present an analysis (the first to our knowledge) of the relative contribution of sea ice processes controlling the mass balance in the pack ice and MIZ, and how this may change in the near future in a warming Arctic. This motivates the use of a sea ice model with a higher physical fidelity than used by climate models ~~and~~ that is able to capture the distinction of MIZ processes. We use ~~a local (CPOM) version of the CICE sea ice model~~ the dynamic-thermodynamic model CICE coupled to a mixed layer model (Petty et al., 2014), ~~which is forced by atmospheric reanalysis and an ocean climatology. This model includes various refinements to the physics (Schröder et al., 2019) and in particular includes a prognostic floe distribution (FSD) model, which is important in realistically representing processes in the MIZ where there is a higher concentration of smaller ice floes. We use a FSD model based on Roach et al. (2018, 2019) that includes brittle fracture (Bateson et al., 2022), found to give realistic simulations of observed FSD for mid-range floe sizes in the Arctic. Using a forced sea ice-mixed layer model does mean that there will be no feedbacks to the atmosphere. There will also be no impact of trends in oceanic properties, such as the "Atlantification" of the Arctic as the subsurface Atlantic Water layer becomes warmer and thicker (Grabon et al., 2021), which has the potential to cause sea ice loss if the heat reaches the surface (Carmack et al., 2015; Onarheim et al., 2014; Polyakov et al., 2013). However, field observations indicate that the majority of the ocean heat needed to explain basal ice melt rates can be explained from solar radiation (Perovich et al., 2011), something our model will suitably capture. Note that using coupled and climate models introduces its own set of problems, e.g. CMIP6 models fail to simulate a realistic seasonal cycle of sea ice area (Notz and Community., 2020). Using a forced sea ice model allows us to simulate a more realistic sea ice state, which has been shown to affect the balance of sea ice processes (Holland et al., 2010; Kee~~ the version we use is described in more detail in Section 2.1. The model has been used in a number of previous modelling studies including Schröder et al. (2019), Rolph et al. (2020), Bateson et al. (2020).

~~In this study we carry out comparisons between different time periods. Between the 1980s where there is a relatively small summer MIZ and the 2010s where there is a large summer MIZ. Then between the 2010s and the 2040s, when the summer sea ice cover is almost entirely MIZ. We quantify the ice volume budget in the different periods, in particular studying the region that becomes MIZ in each of the comparisons to investigate the changes in the volume budget as the MIZ expands. The terms of the sea ice volume budget we examine are:~~

- ~~**Congelation** growth - basal thickening of the sea ice which occurs from autumn until spring~~
- ~~**Frazil** ice formation - supercooled seawater freezes to form frazil crystals which clump together to create sea ice~~

- **Snowice** - snow ice formed when the snow layer on top of the sea ice is pushed below water, is flooded and freezes
- **Basal melting** - melting at the base of the sea ice
- **Top melting** - melting on the surface of the sea ice, which may form melt ponds
- **Lateral melting** - melting at the edge of the sea ice floes
- **Sublimation** - sublimation from the surface of the sea ice. In this study this term includes snow sublimation
- **Dynamics** - the sum of advection, convergence and ridging. This redistributes the ice and can cause either loss or gain of sea ice in a given region. This occurs all year round

The structure of this paper is as follows. The sea ice-mixed layer model is described in Section 2.1. The NCEP and HadGEM2-ES forced simulations are compared to satellite observations and PIOMAS ice volume estimates in Section **??**, the atmospheric forcing used is described in Section 2.2, the simulation is compared to data which is outlined in Section 2.1 and used to validate the simulated sea ice extent and volume in Sections 2.2 and 2.3, followed by a description of the analysis method in Section 2.1. The ice volume fluxes in the pack ice and MIZ in low MIZ *low MIZ* (1980s), high MIZ *high MIZ* (2010s) and all MIZ *all MIZ* (2040s) scenario are compared in Section 3. The total annual fluxes are shown in Section 3.1 followed by the annual cycle in the main melt and growth terms in Section 3.2. Finally the main findings We present our Discussion in Section 4 and, finally, the main results are summarised in the Concluding remarks in Section 5.

2 Methodology

2.1 Model set up and ocean forcing

We use a dynamic-thermodynamic sea ice model, CICE coupled to a mixed layer model of Petty et al. (2014). We use the (Petty et al., 2014), which is forced by atmospheric reanalysis (detailed in Section 2.2) and an ocean climatology. We used the local CPOM version of CICE which is based on version 5.1.2 (Hunke et al., 2015). This version has been calibrated to model includes various refinements to the physics, including calibration to Cryosat-2 data (Schröder et al., 2019). This version of CICE uses , the form drag scheme of Tsamados et al. (2014) and a joint prognostic floe size distribution (FSD) model(Roach et al., 2018, 2019) that includes a parameterisation of and thickness distribution (FSTD) model, which is important in realistically representing processes in the MIZ where there is a higher concentration of smaller ice floes. We use a FSTD model based on Roach et al. (2018, 2019) that includes brittle fracture (Bateson et al., 2022). The addition of this brittle fracture parameterisation improves model performance in simulating the shape of the FSDfor mid-sized floes. Examples of previous use of the CPOM version of the CICE modelare demonstrated in Rolph et al. (2020) without the addition of brittle fracture in the prognostic FSD model, and in Schröder et al. (2019) without a prognostic FSD model or prognostic mixed layer model, found to give realistic simulations of observed floe size distributions (FSD) for mid-range floe sizes in the Arctic. This model,

minus the brittle fracture addition to the FSTD model, has been used previously by Rolph et al. (2020) to compare changes in the MIZ in a sea ice model to satellite observations.

We run the model in standalone mode for the pan-Arctic, with a grid resolution of ~40 km. The ocean temperature and salinity below the mixed layer are restored to climatological means from ~~MYO-WP4-PUM-GLOBALREANALYSIS-PHYS-001-004~~ the MyOcean global ocean physical reanalysis product (Ferry et al., 2011) over a time scale of 20 days. The ocean currents are restored to values from the same dataset, also over 20 days. The mixed layer temperature, salinity and depth are calculated based on heat and salt fluxes from the deeper ocean and the atmosphere/ice at the surface. We use a number of the default CICE settings including seven vertical ice layers, one snow layer, thermodynamics of Bitz and Lipscomb (1999), Maykut and Untersteiner (1971) conductivity, the Rothrock (1975) ridging scheme with a Cf value of 12 (an empirical parameter that accounts for dissipation of frictional energy), the delta-Eddington radiation scheme (Briegleb and Light, 2007), and the linear remapping ice thickness distribution (ITD) approximation (Lipscomb and Hunke, 2004). Additionally we use a prognostic melt pond model (Flocco et al., 2010, 2012) ~~,~~and an anisotropic plastic rheology (Heorton et al., 2018; Tsamados et al., 2014; Wilchinsky and Feltham, 2006)~~and a prognostic floe size distribution model (Roach et al., 2018) that includes brittle fracture (Bateson et al., 2022). ~~. We used the same wave forcing set up as Bateson et al. (2022). Note that this is a different set up to Roach et al. (2019) where a separate wave model is coupled to the sea ice model to calculate the wave properties in the grid cells that contain sea ice. Instead, we use an extrapolation method as used and documented in Roach et al. (2018), where ERA-I wave forcing (Dee et al., 2011) is used to calculate the necessary in-ice wave properties. The wave forcing consists of the significant wave height and peak wave period for the ocean surface waves. These fields are updated every 6 hours in the grid cells that contain less than 1% sea ice. Crucially for this study, despite not having a coupled wave model our set up still enables wave induced fracture causing enhanced lateral melting and wave-dependent new ice formation, as outlined in Roach et al. (2019). After 2017 we repeat the wave forcing, which does mean there is no trend in the wave forcing. Sensitivity studies varying the wave forcing using this model have demonstrated limited sensitivity to the wave forcing (Bateson, 2021) and comparisons to future 2056-2060 climatology from a global RCP8.5 wave simulation shows no significant change in significant wave height or interannual variability in significant wave height (Bateson, 2021). Although the wave forcing fields do not have any trends, the propagation of the waves into the ice field does respond to the changes in the ice cover over time. The simulations were initialised with a 6 year spin up period, this is a similar length to previous studies using the same model setup (Rolph et al., 2020; Bateson et al., 2022). As we are using a standalone sea ice model, the amount of spin-up required is much shorter than a climate simulation, or a coupled sea ice-ocean model.

~~We use~~

2.2 Atmospheric forcing data

We used two atmospheric forcing sets, NCEP Reanalysis-2 (NCEP2) (Kanamitsu et al., 2002, (updated 2017) atmospheric forcing from 1979 to 2020 and HadGEM2-ES (RCP8.5) (Jones et al., 2011) forcing from 1980 to 2050. Surface air temperature, wind speed and specific humidity is updated every six hours in the model, incoming shortwave and longwave radiation every 12 hours and monthly averages are used for precipitation. The HadGEM2-ES product is purely model based (no data assimilation)

and is included to allow us to consider a projection into the mid twenty first century, which enables us to study changes as the summer sea ice cover becomes entirely MIZ. We used the first member of the 3 member ensemble. HadGEM2-ES has been shown to simulate a realistic Arctic sea ice cover (Wang and Overland, 2012), making it a suitable choice. As we would expect the NCEP data set to be closer to reality due to it being a reanalysis, we treat the NCEP forced simulation as a check and a comparison for the HadGEM2-ES simulation and results in this study.

The surface air temperatures are significantly higher in the NCEP reanalysis than HadGEM2-ES between December to early April in both the 1980s and 2010s period, as shown in Figure 1a. For the rest of the year they are more comparable, apart from the HadGEM2-ES forcing being slightly warmer in October and November. The largest warming is seen from September though the Autumn. Looking at the change in annual average values in Figure 2 we can see that between the 2010s and 1980s NCEP and HadGEM2-ES warms by roughly 2°C across the central Arctic. The warming continues at a similar pace in the HadGEM2-ES to the 2040s, with warming of typically 8°C across the central Arctic from the 1980s, including near the Canadian archipelago, where warming was slightly lower in the 2010s. The humidity values shown in Figure 1b are relatively similar in the NCEP and HadGEM2-ES forcing sets, with higher humidity values in the NCEP forcing set during the December-early April period. The trend over time in both data sets is increasing humidity in all months, particularly from July through until December. The shortwave and longwave radiation values are very different between the two data sets, as shown in Figures 1c and d. NCEP has much higher summer shortwave radiation values, whilst HadGEM2-ES has much higher year round longwave radiation values, but particularly summer values. It is likely that this dramatic difference is due to differences in cloud cover.

3 Simulated and observed sea ice extent and volume

Here the

2.1 Model validation data

Rolph et al. (2020) compared a very similar model set up to ours with a number of different satellite observational products. Here we compare our simulated sea ice extent and volume from the NCEP and HadGEM2-ES forced simulations are compared alongside extent from satellite observations, in Section 2.2, and ice volume from MIZ extent with NASA Team (Cavalieri et al., 1996) and NASA Bootstrap (Comiso, 2017). We chose to do this due to the large observational spread of MIZ extent estimates found in Rolph et al. (2020). NASA Team has a MIZ extent on the higher end of observational estimates whilst NASA Bootstrap is on the lower end. The two products gives us an estimate of the large range of MIZ extent suggested by satellite products. In both cases, the SIC values were interpolated onto the ORCA tripolar 1° grid which is used by the CICE model. The CICE land mask was applied and the pole hole was filled with 98% SIC, which was consistent with the surrounding values in the datasets. Daily values are used to compute monthly values of sea ice and MIZ extent that are plotted in Figure 3.

PIOMAS, the Pan-Arctic Ice Ocean Modeling and Assimilation System (PIOMAS) (Zhang and Rothrock, 2003) , in Section 2.3. (Zhang and Rothrock, 2003) is a model that assimilates a range of sea ice area/concentration observations to give an

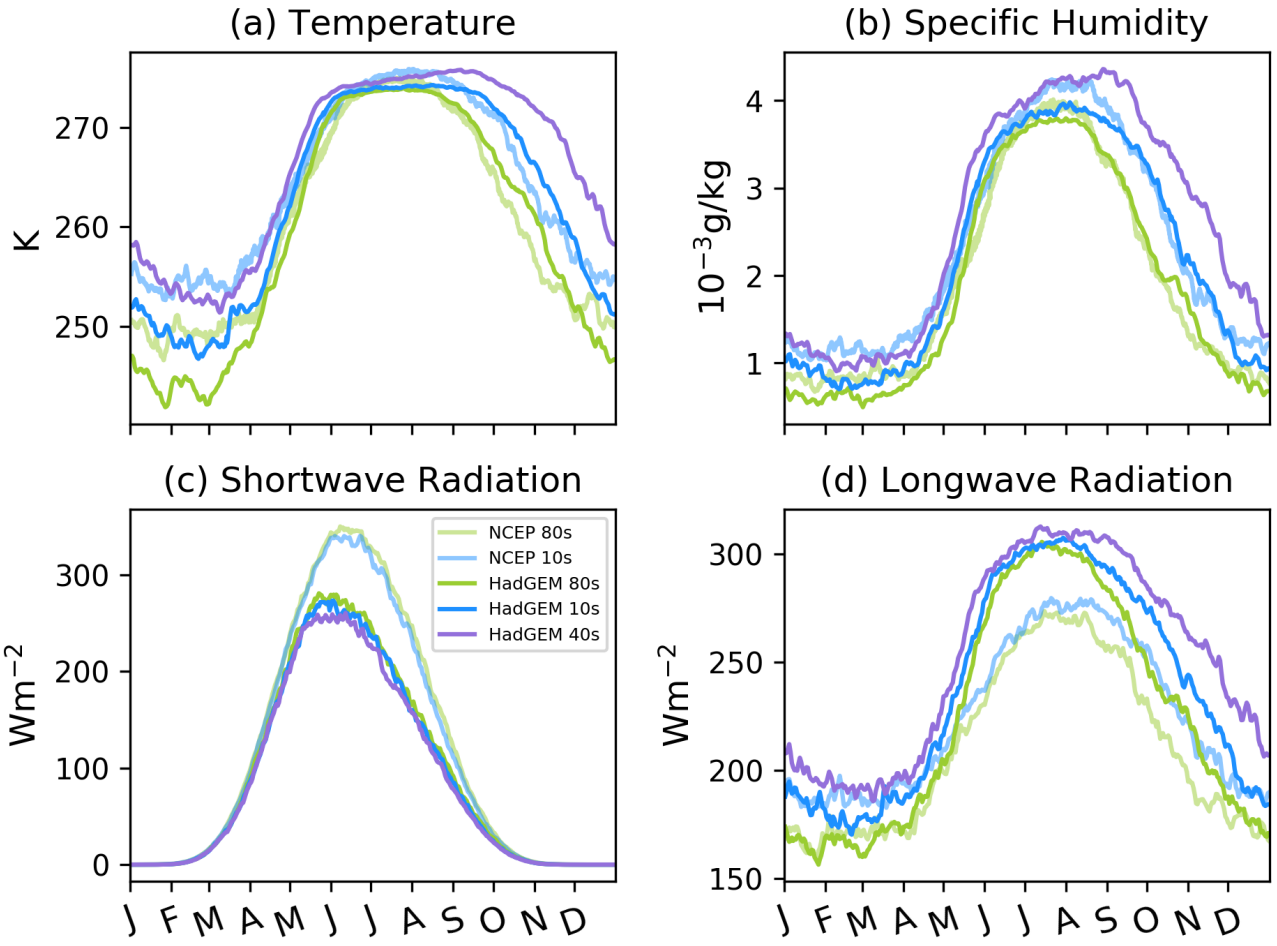

Figure 1. NCEP and HadGEM2-ES atmospheric forcing, a) surface air temperature, b) specific humidity, c) shortwave radiation and d) longwave radiation are shown for the 5 year study periods during the 1980s, 2010s and 2040s as outlined in Section 2.1, over ocean north of 66.5°N.

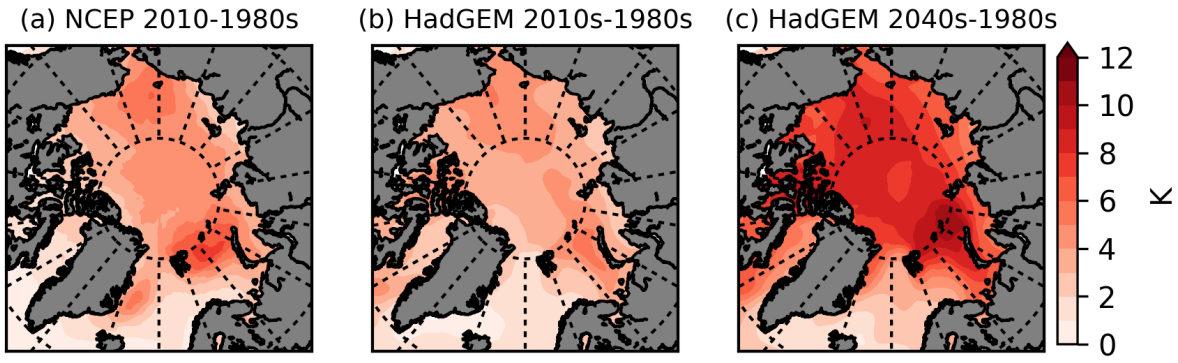

Figure 2. NCEP and HadGEM2-ES warming between the 5 year study periods. a) 2010s-1980s (NCEP), b) 2010s-1980s (HadGEM2-ES) and c) 2040s-1980s (HadGEM2-ES). The differences are between the annual average temperatures.

estimate of continuous Arctic sea ice volume changes over time. Satellite observations have given us continuous sea ice concentration and extent estimates since 1979, but sea ice thickness and volume are more difficult, particularly in summer when there are lots of melt ponds. The continuous nature of the PIOMAS estimates, and the pan-Arctic coverage, make it a useful comparison for this modelling study. As with the satellite data, PIOMAS has been interpolated on the ORCA tripolar 1° grid and the CICE land mask has been applied.

2.2 Sea ice and MIZ extent

The NCEP forced simulation spans from 1979 to 2020, whilst the HadGEM2-ES simulation spans from 1980 to 2050. ~~Both were initialised with a 6 year spin up period. The minimum and maximum sea ice extent~~ The monthly sea ice and MIZ extent ~~for each simulation and period studied is given in Table **??**. The values are calculated from the average annual cycle of sea ice /MIZ extent of the last 5 years of each decade in~~ values for June, July, August and September are given in Figure 3, alongside values from NASA Team and Bootstrap (see Section 2.1). The two simulations are relatively similar to each other, the NCEP forced simulation has a consistently lower sea ice extent over the historical period in June (Figure 3), but this difference decreases in the other summer months. The simulated sea ice extent in the ~~simulations. The period of 5 years was chosen in order to try to capture particular MIZ states in the simulations without averaging over larger windows. We chose the last 5 years of the 1980s, 2010s and 2040s to reflect a *low MIZ state*, *high MIZ state* and *all MIZ state* in the simulations. The maximum~~ forced atmosphere simulations compare well to the satellite observations from NASA Team and Bootstrap. The simulations show a slighter weaker sea ice trend in June and July (Figure 3a&b), whilst being slightly lower, but very similar to the satellite observations in August and September (Figure 3c&d).

Whilst the sea ice extent ~~is the same in both simulations in the 1980s, and similar in the 2010s,showing a relatively modest decline from 1.22×10^7 km^2 in the 1980s to 1.15×10^7 km^2 in the 2040s in the HadGEM2-ES forced simulation. The NCEP forced simulation shows a stronger declining~~ observations are generally in relatively good agreement, satellite observations show a large range of estimates for the MIZ (Rolph et al., 2020). The interannual variability in the MIZ extent in both simulations and observations in July, August and September (Figures 3b,c&d) is large. NASA Team and Bootstrap do not show a trend in the MIZ extent in any month, though because of the decreasing trend in summer sea ice extent ~~trend than the HadGEM2-ES forced one, which can be seen in~~ the fraction of the sea ice ~~extent minima values . In the~~ cover that is MIZ increases. The simulations show an increasing trend in July and August (Figures 3b&c), starting off close to the Bootstrap MIZ extent values in the 1980s, and ending up closer to the NASA Team values in the 2010s. In 2010s the MIZ has become the dominant part of the sea ice cover in July, August and September. By the end of the 2030s the sea ice cover has become almost entirely MIZ in August and September and in the 2040s the ~~minimum~~ sea ice extent in August and September goes below the value commonly used to define the Arctic as ~~seasonally~~ ice free (1×10^6 km^2).

~~In Figure 3 we compare the two simulations to each other and satellite observations from NASA Team and NASA Bootstrap, which we chose to give an upper and lower estimate of MIZ extent values from satellite observations. The Bootstrap and NASA Team~~ Comparing the averaged sea ice extent and MIZ extent in the two study periods (Figure 4a&b) shows that both forced simulations overestimate winter sea ice extent~~estimates are very similar to each other. Generally the~~ , this bias increases in the

2010s due to the larger drop in winter sea ice extent ~~is slightly lower~~ in the satellite observations ~~in June and July and slightly higher in August and September. The sea ice extent is generally lower in the NCEP forced simulation than the HadGEM2-ES forced simulation, with lower MIZ extent, especially in August and September. NASA Team gives us an upper estimate of MIZ extent, whilst Bootstrap gives us a lower estimate. The simulations start off generally closer to the lower estimate (Bootstrap)~~ from the 1980s to the 2010s. The simulations are in relatively good agreement with NASA Team and NASA Bootstrap in the summer months~~with the exception of the HadGEM2-ES forced simulation in August and September. The simulations then tend more towards the upper estimate (NASA Team) in July, August and September months. This is due to the increasing MIZ extent trend present in the simulations which is not in the observations. Despite this discrepancy, the forced simulations fall within the observational estimates which gives us confidence that they are simulating an appropriate sea ice state and are suitable for this study. There~~ , showing slightly lower minima. From Figure 4c&d we can see there is a large increase in the MIZ extent in the NCEP forced simulation moving from the 1980s to the 2010s. From Figure 4c&d we can see there is a large ~~range in summer MIZ estimates between different satellite products, as discussed in Rolph et al. (2020). Both simulations are on the lower end of estimates in June, and the upper end in July and August when the MIZ peaks. By the 2010s~~ increase in the MIZ ~~becomes the dominant part of the Arctic sea ice cover in the simulations and observations, and by the end of the 2030s the summer sea ice cover is almost entirely MIZ in the HadGEM2-ES forced simulation~~extent in the NCEP forced simulation moving from the 1980s to the 2010s. The MIZ extent values from NASA Team and NASA Bootstrap show little change, however the simulations stay reasonably close to the range the satellite observations suggest.

~~1.22×10^7 km^2 1.22×10^7 km^2 1.21×10^7 km^2 1.19×10^7km^2 1.15×10^7km^2~~

~~6.30×10^6km^2 5.94×10^6km^2 2.50×10^6km^2 2.81×10^6km^2 3.15×10^5km^2~~

~~2.03×10^6km^2 3.99×10^6km^2 4.58×10^6km^2 4.75×10^6km^2 6.46×10^6km^2 8.82×10^5km^2 7.42×10^5km^2 7.96×10^5km^2 7.07×10^5km^2 1.74×10^5km^2~~

~~Table of sea ice extent and MIZ extent minimum and maximum values for each time period. In each case the last 5 years of sea ice extent in each decade has been averaged and the minimum and maximum sea ice extent and MIZ extent is values for sea ice and MIZ extent is calculated from the averaged annual cycle.~~

~~Monthly June, July, August and September sea ice (solid lines) and MIZ extent (dashed lines) from the NCEP (1979-2020) and HadGEM2-ES (1980-2050) forced simulations compared to satellite observations from NASA Team (1979-2020) and NASA Bootstrap (1979-2020). Yellow shaded areas show the three study 5 year periods used in Section 3.~~

2.3 Sea ice volume

~~Total~~ Here we compare the total sea ice volume over the Arctic ~~ocean (defined here as being ocean North of 66.5°N) is plotted for~~ Ocean from the HadGEM2-ES and NCEP forced simulations alongside monthly values from PIOMAS~~in Figure 5. The NCEP forced model is relatively similar to the PIOMAS estimate, showing similar variability, but~~ . In Figure 5a, we can see that the NCEP forced simulation overestimates the seasonal cycle, mostly due to too much sea ice volume in the winter but is nonetheless relatively similar to the PIOMAS estimate (difference plot in Figure 5b), showing similar variability. Meanwhile the HadGEM2-ES forced simulation underestimates the sea ice volume all year round (Figure 5a), although it does tend towards

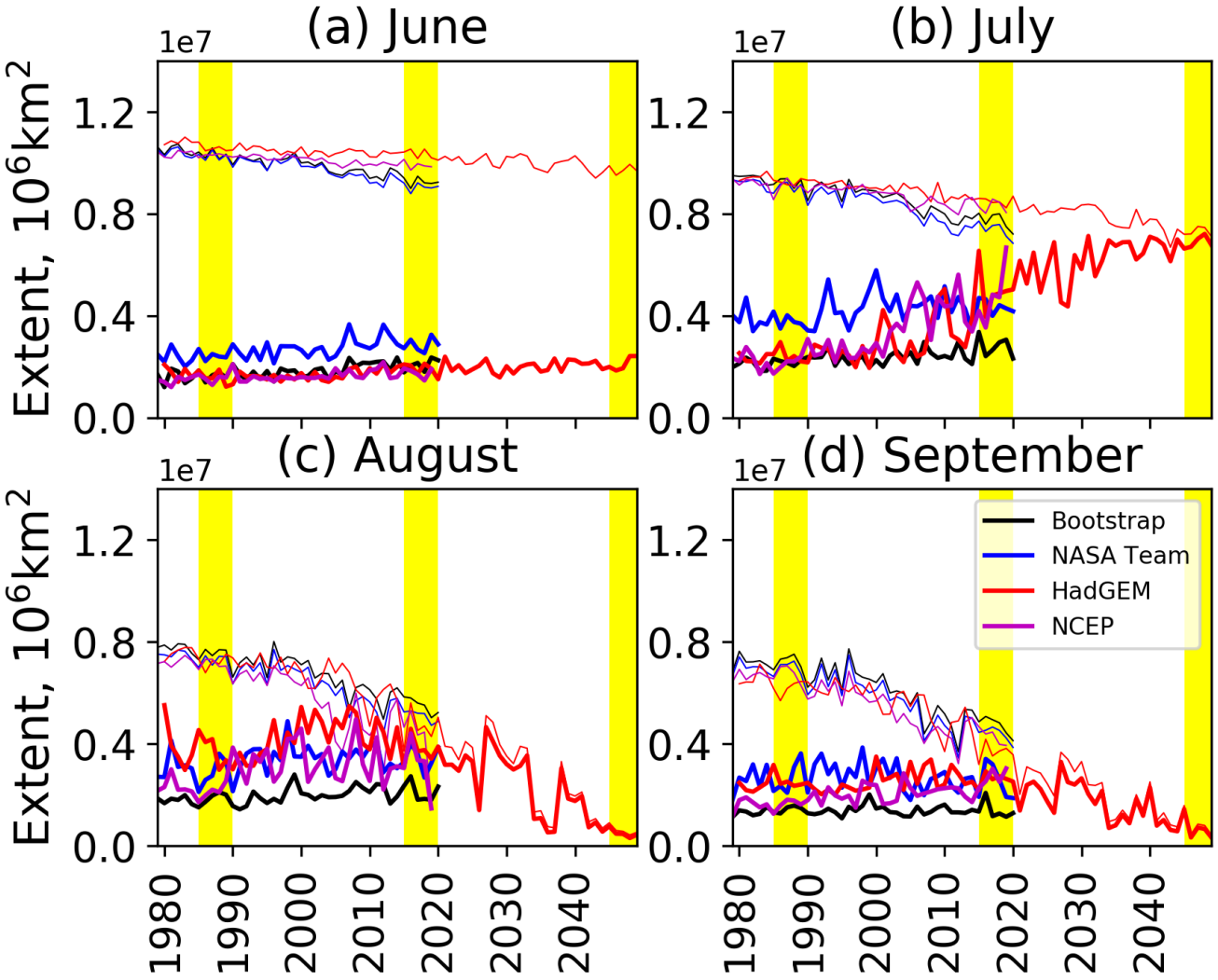

Figure 3. Monthly June, July, August and September sea ice (thin lines) and MIZ extent (thick lines) from the NCEP (1979-2020) and HadGEM2-ES (1980-2050) forced simulations compared to satellite observations from NASA Team (1979-2020) and NASA Bootstrap (1979-2020). Yellow shaded areas show the three study 5 year periods used, see Section 2.1. Uncertainty levels of $+/-10\%$ were used for the satellite values in Rolph et al. (2020), they have been left out in these figures to make them clearer.

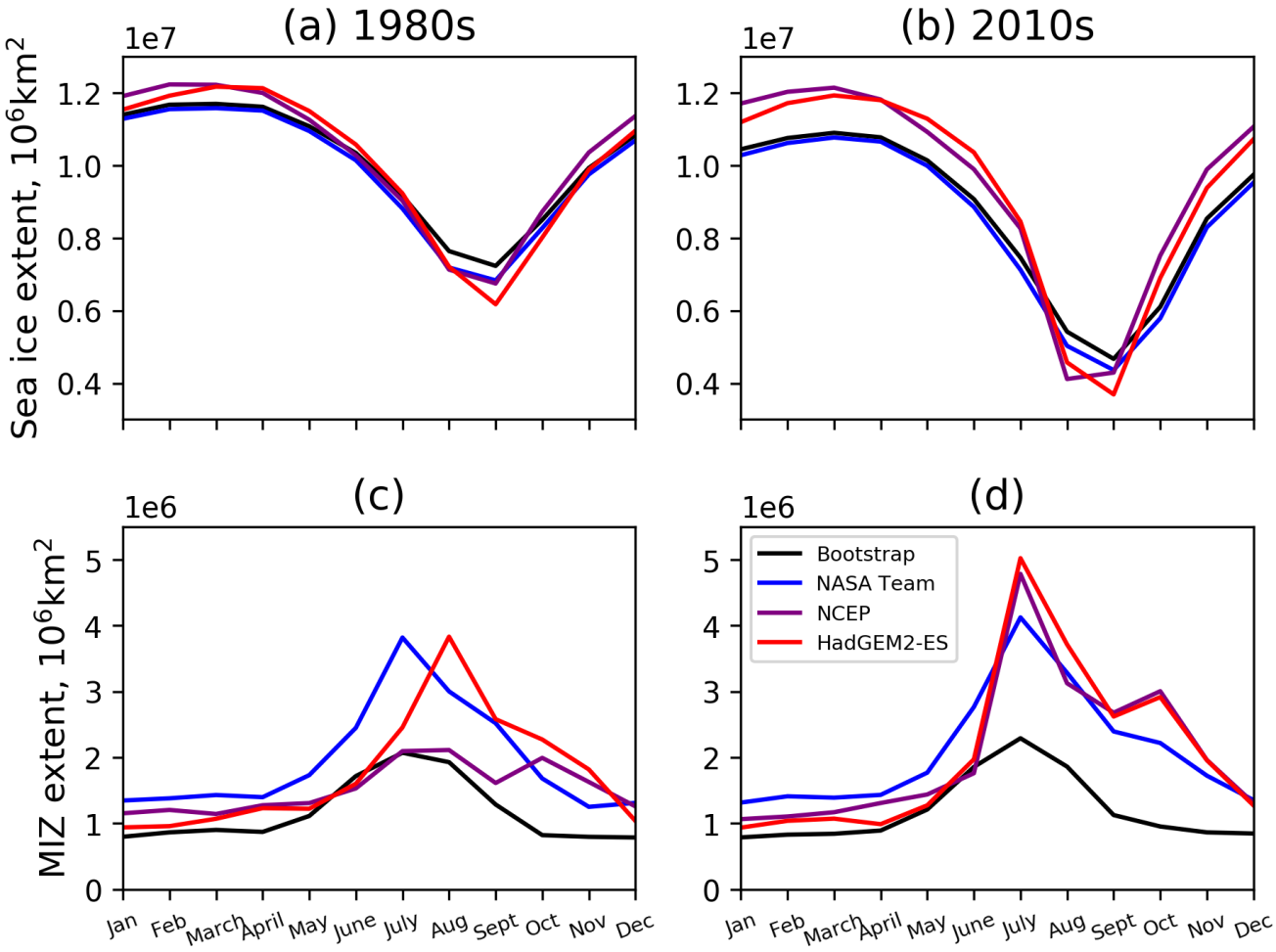

Figure 4. Monthly values of sea ice extent and MIZ extent over 1985-1990 and 2015-2020 or the NCEP and HadGEM2-ES forced simulations and satellite observations from NASA Team and NASA Bootstrap.

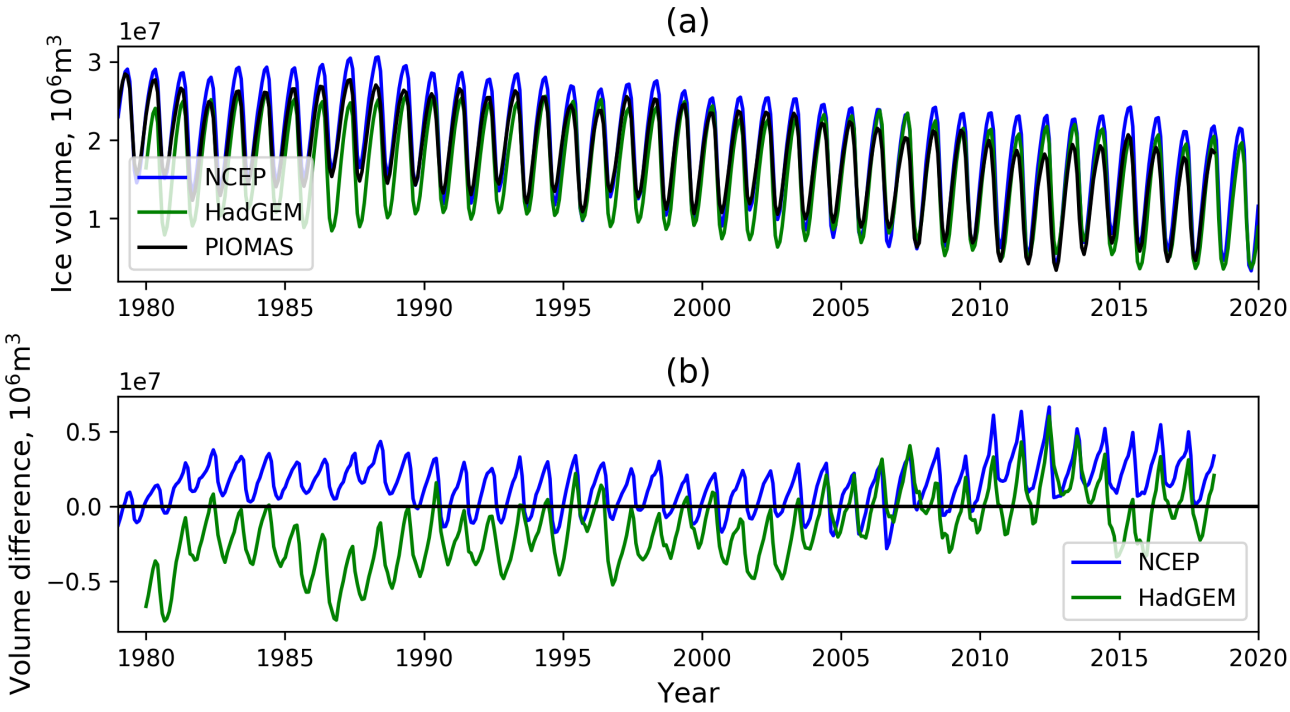

Figure 5. Monthly Arctic sea ice volume from NCEP and HadGEM2-ES forced simulations compared to PIOMAS in (a) and the differences from PIOMAS shown in (b).

to the PIOMAS estimate over time (Figure 5b) due to showing a smaller sea ice volume decrease over time. Both simulations produce suitably realistic sea ice extent and volume for use in this study.

3 ~~Results: Volume fluxes in the pack ice and MIZ~~

2.1 Analysis Method

~~Here we compare the sea ice volume fluxes in the pack ice and MIZ. The MIZ is taken to be between 15-80% sea ice concentration whilst the pack ice is taken to be regions of sea ice concentration above 80%.~~ We consider three different ice cover states within the simulations: a *low MIZ state* in the 1980s; a *high MIZ state* in the 2010s; and an *all MIZ state* in the 2040s. Figure 6 shows the change in MIZ coverage in the summer based on daily July ~~sea ice concentration~~ SIC fields from the two simulations plus NASA Team and NASA Bootstrap from the 1980s to the 2010s, and then from the 2010s to the 2040s from the HadGEM2-ES forced simulation. In each case we use the last 5 years of daily July ~~sea ice concentration~~ SIC and assign each grid cell as pack ice (~~ice concentration~~SIC$\geq$80%), MIZ (15% $\leq$~~ice concentration~~SIC$<$80%) or open water (~~ice concentration~~SIC$<$15%). We then compute where a grid cell spends most of its time in each time period to define each region

as pack ice, MIZ or open water. This gives a more accurate representation of where the MIZ is observed and simulated than computing the MIZ from time averaged ~~sea ice concentration~~ SIC fields. The use of fixed regions for our analysis means that they do not reflect what is MIZ and pack ice on each day of the year, however it does enable us to analyse volume fluxes in the region that is predominantly MIZ in July.

Region 1, *always pack ice* (blue in Figure 6), is the area that was pack ice in both the 1980s and 2010s (2010s and 2040s); region 2, *becomes MIZ* (green), is the area that was pack ice in the 1980s (2010s) and became MIZ in the 2010s (2040s); and region 3, *always MIZ* (orange), is the region that was MIZ in both the 1980s and 2010s (2010s and 2040s).

There is a large range in the MIZ coverage estimated by satellite products ~~Rolph et al. (2020), we~~ (Rolph et al., 2020). We chose Bootstrap and NASA Team for this comparison to give an indication of lower and upper observational estimates of MIZ extent. NASA Team has a much larger region that *becomes MIZ* and is *always MIZ* than Bootstrap. The MIZ coverage in the NCEP and HadGEM2-ES forced simulations is closer to Bootstrap in the 1980s and closer to NASA Team in the 2010s as given in ~~Table ??~~Figure 7. The simulations show a different spatial coverage to the MIZ and changes compared to the satellite observations. The simulations show a larger increase in the MIZ around the Fram Strait region, particularly in the HadGEM2-ES forced simulation. There is a similar change in percentage of MIZ coverage in the two simulations, with the HadGEM2-ES forced simulation showing slightly more MIZ in both periods. By the 2010s the MIZ is making up 46%/50% of the July sea ice cover in the NCEP/HadGEM2-ES forced simulations, and 93% by the 2040s in the HadGEM2-ES forced projection ~~.~~(see Figure 7).

We analyse the simulated annual volume fluxes in Section 3.1 and annual cycles for the melt terms and congelation growth in Section 3.2 using the regions defined in Figure 6. The terms of the sea ice volume budget we examine in each simulation for each region and time period are:

- **Congelation** growth - basal thickening of the sea ice which occurs from autumn until spring
- **Frazil** ice formation - supercooled seawater freezes to form frazil crystals which clump together to create sea ice
- **Snowice** - snow ice formed when the snow layer on top of the sea ice is pushed below water, is flooded and freezes
- **Basal melting** - melting at the base of the sea ice
- **Top melting** - melting on the surface of the sea ice, which may form melt ponds
- **Lateral melting** - melting at the edge of the sea ice floes
- **Sublimation** - sublimation from the surface of the sea ice. In this study this term includes snow sublimation
- **Dynamics** - the sum of advection, convergence and ridging. These processes redistributes the ice and can cause either loss or gain of sea ice in a given region. This occurs all year round.

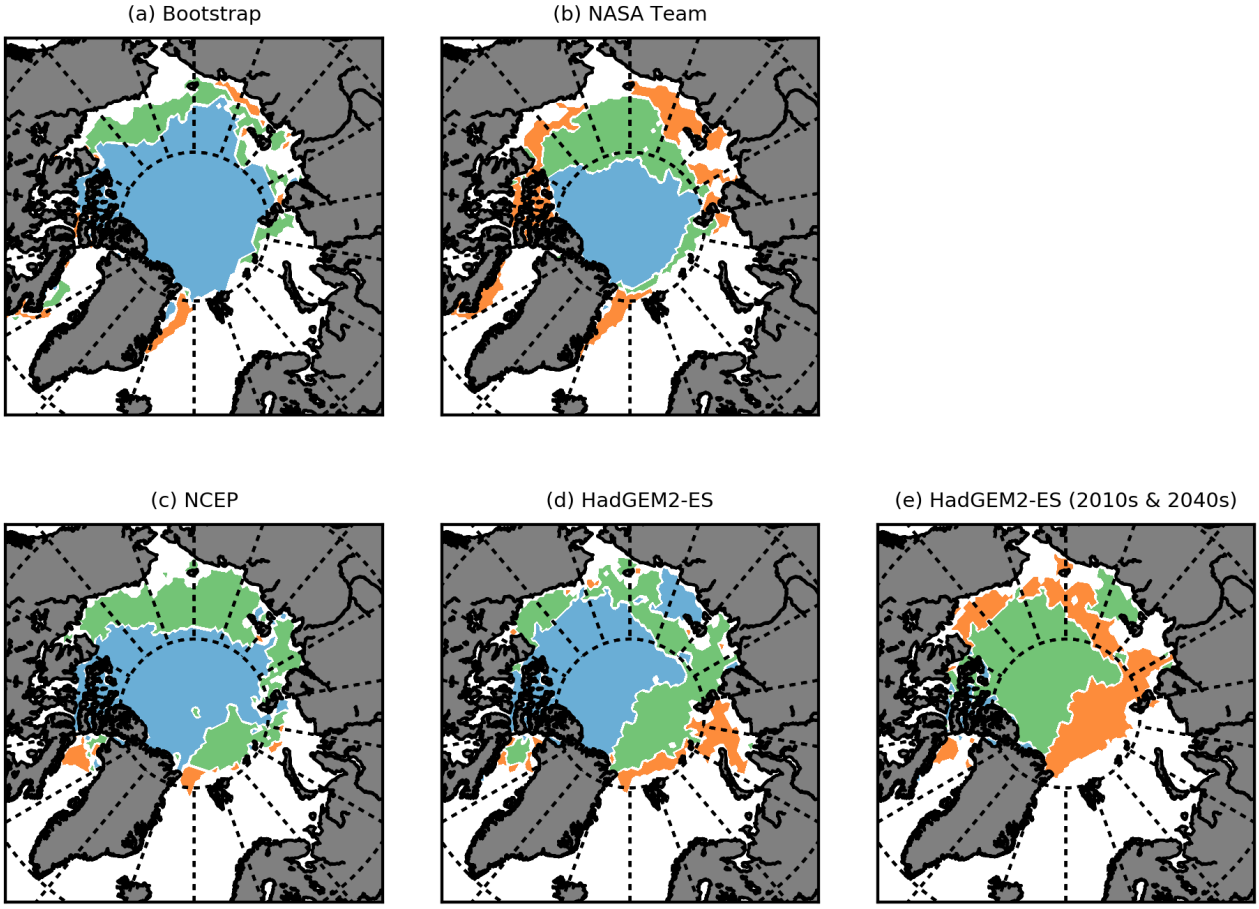

Figure 6. Regions of the Arctic sea ice cover defined from daily July ice concentration fields from each time period from the NCEP and HadGEM2-ES forced simulations. Region 1 (blue) indicates the area that is pack ice in both the 1980s(2010s) and 2010s(2040s) in subplots a-d(e). Region 2 (green) indicates the area that is pack ice in the 1980s(2010s) and becomes MIZ in the 2010s(2040s) in subplots a-d(e). Region 3 (orange) indicates the area that is MIZ in both the 1980s(2010s) and the 2010(2040s) in subplots a-d(e).

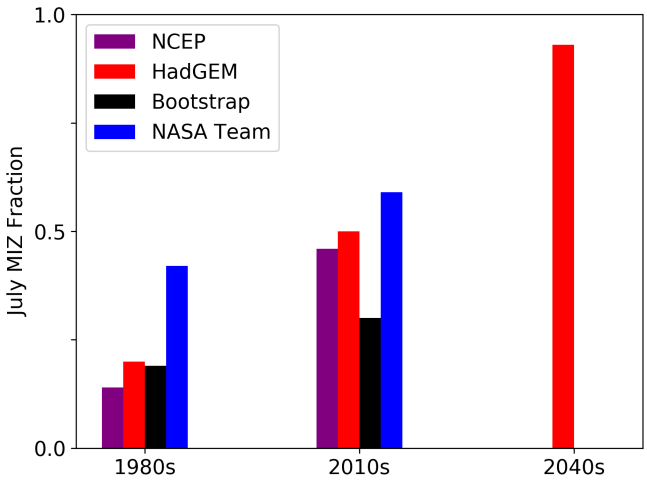

Figure 7. Fraction of the July sea ice cover that is MIZ in each study period from the two forced CICE simulations and NASA Bootstrap and NASA Team (see Section 2.1).

3 Results: Volume fluxes in the pack ice and MIZ

3.1 Annual total volume fluxes

Here we discuss the The annual volume fluxes for sea ice processes as are shown in Figure 8and the relative importance of top, basal and lateral melting in the 1980s as shown in Figure ??. Congelation growth dominates sea ice growth making up between 91-95% in both pack ice and MIZ regions with no clear change over time or contrast between the pack ice and MIZ in Figure 8. Frazil is the next biggest ice growth term making up between 5-9%. In all cases snow ice formation is a negligible contribution to sea ice growth making up less than 1% in all periods and regions. This growth partitioning applies to both the NCEP and HadGEM2-ES forced simulation; there are some small changes over time in each region as shown in Figure 8, but not outside the range stated above.

The partitioning of the melt between top, basal and lateral melting does differ significantly substantially between the pack ice and MIZ, as shown in Figure 9, although there is broad consistency between the two forced simulations over the 1980s and 2010s. In all regions and simulations basal growth in both simulations basal melt makes up the largest proportion of meltingranging between 46-60% in regions of pack ice and 52-69% in regions of MIZ across the simulations and time periods, and is generally slightly higher in the MIZ regions, particularly the *always MIZ* regions. In the 1980s and 2010s simulations (Figures 9-f) top melting is significantly substantially more important in the pack ice than in the MIZ, this is predominantly compensated by an increase in lateral melting in making up roughly twice as much of the melting in the region of *always pack ice* compared to the region of *always MIZ*. The opposite is true for lateral melting, the fraction of melting in regions of *always MIZ* are more than twice the fraction in the MIZ alongside an increase in basal melt in the MIZ relative to the pack. Top melt

~~makes up 39-50% in the *always pack* region and 15-21%~~ regions of *always pack ice*. This makes the fraction of top and lateral melt comparable in the *always MIZ* region~~in the~~ , particularly in the NCEP simulation.

There is very little change in the melt fractions between the 1980s and the 2010s. ~~Whilst the~~ The largest change is in the ~~*becomes MIZ*~~*always pack ice* ~~values are intermediate to the other two regions with top melt making up 30-36%. Lateral melting makes up 4-5% of melting in the *always pack* region, 6-9%~~ region, where there is a slight decrease in top melt and a compensating increase in the fraction of basal and lateral melting. This indicates a tendency towards the values seen in the *becomes MIZ* region~~and 10-15% in the *always MIZ* region.~~

. It is surprising that there is not a more significant change ~~over time~~ in the *becomes MIZ* region ~~which is pack ice in the 1980s(2010s) and MIZ in the 2010s(2040s) in~~ over time in terms of proportion of melt that is top, basal or lateral ~~. The~~ (see Figure 9). It might have been expected that balance would have shifted between the two time periods. Instead, the values are approximately midway between those of the *always pack ice* and *always MIZ* regions. ~~This likely reflects that the contrasts between the pack ice and the MIZ regions are sensitive to the sea ice concentration gradient and associated properties, as opposed to the binary classification of pack ice or MIZ. This means that it is likely that MIZ closer to the pack ice has a different balance of processes to the outer MIZ that has lower ice concentrations.~~

The top, basal and lateral melt fractions in the ~~projections~~ projection to the 2040s do not match the earlier period in the HadGEM2-ES forced simulation. There is much more top melting in both the *always MIZ*, and to a lesser degree the *becomes MIZ* region. This result is consistent with the increase in top melting seen in the near future in CMIP6 model projections (Keen et al., 2021). This is likely driven by the warming seen in the surface air temperature in the atmospheric forcing, as shown in Figures 1 & 2. The changing location of the sea ice might be a partial explanation of the change, as the sea ice moves to higher latitudes this may have an impact on the balance of processes~~in addition to whether the sea ice is located in the pack ice or MIZ. A possible explanation for the increase in top melting in the future MIZ simulated could also be the use of constant ocean forcing in the projection, which may be lacking ocean warming and therefore not represent realistic ocean conditions for the projection. This means that the results here could be seen as a lower estimate on the ice loss and changes that we will expect to see in the 2040s depending on the speed and~~ , particularly as this is where there is generally a greater magnitude of warming~~of Atlantic Waters entering the Arctic Ocean. Feedbacks with the atmosphere may also act to speed up and intensify the changes in ice and temperature that we might expect to see in the 2040s~~.

Dynamics (advection ~~, convection and ridging~~and convergence) results in a net negative flux in all regions, though the magnitude is significantly larger in the pack ice than in the MIZ as might be expected due to a larger volume of sea ice that can be advected. These results reflect that generally sea ice is exported outwards from the central Arctic and melts at lower latitudes. ~~In all of the regions the magnitude of the negative dynamics sea ice flux decreases over time, reflecting the reduction in sea ice volume. In the NCEP simulation the decrease in negative volume flux in the 2010s~~ This means that dynamics plays a more significant role in ice loss in the *always pack* region, roughly 30%, whilst this decreases relative to the ~~1980s was relative similar in all of the regions, ranging 31-34%. In the HadGEM2-ES forced simulation more of a contrast across the regions , with a larger~~ amount of melt in the *becomes MIZ* and *always MIZ* regions. In all regions there is a strong decrease in the ~~MIZ likely reflecting larger ice loss . With a decrease of 31% in the *always pack* region, 43% decrease in the *becomes MIZ*~~

~~region and 51% in the always MIZ region. In the the projection the change from the 2010s to~~ proportion of ice loss that is due to dynamics, the ~~2040s we see a continuation of the prior changes, with a 48% decrease in the~~ largest change occurring in the NCEP *always pack ice* region. Dynamics is comparable to lateral melting in the *becomes MIZ* region, much larger in the ~~*becomes MIZ*~~*always pack* region and ~~a 41% decrease~~ smaller in the *always MIZ* region.

3.2 Annual cycle of the main melt and growth terms

To better understand the net changes in annual sea ice volume fluxes and investigate changes to the onset and length of melting we looked at the average annual cycle of congelation growth, basal, top and lateral melt fluxes, shown in Figure 10. The same regions and time periods defined in Figure 6 ~~are~~ have been used.

Melting occurs first in the outer regions (*always MIZ* regions) and progresses inwards across the sea ice cover to the *always pack ice* region. This is more pronounced in the NCEP simulation, likely a reflection that the NCEP atmospheric forcing is warmer in summer (see Figure 1a). Top melting occurs first, followed by basal melting in the *always pack ice* and *becomes MIZ* regions. Lateral melting has a less pronounced summer peak that appears later in the melt season (early ~~august~~August) than the other melt terms, reflecting the increase in fragmentation of the sea ice cover as the summer progresses. Lateral melting is a larger melt term in the MIZ regions, as ~~documented~~ noted in the previous section. Melting rates and growth rates (per unit area) are larger in the MIZ than the pack ice in the 1980s in both simulations, this difference decreases in the 2010s as melting and growth fluxes increase in the *always pack ice* region by more than in the *becomes MIZ* and *always MIZ* regions, reflecting the increase in seasonality in the pack ice.

In the *always pack* region peak melt increases and the melt season gets longer in the 2010s relative to the 1980s by 13 days in the NCEP and 6 days in the HadGEM2-ES forced simulations. This is primarily due to earlier melting onset by 9 days in the NCEP and 8 days in the HadGEM2-ES forced simulation. Note here we use $2.5\times10^{-3}\mathrm{m}^3\mathrm{m}^{-2}\mathrm{day}^{-1}$ as the threshold for melting starting and ending to capture the main phases of melt and growth, as opposed to oscillations or lower rates of melting. Peak melting rates increase, particularly in the NCEP simulation where they increase by 49%, compared to a 17% increase in the peak melting rate in the HadGEM2-ES simulation. The difference is likely due to the greater summer surface air temperatures (see Figure 1a) which drives a larger seasonal sea ice cycle (see Figure 5a). This is partially compensated by an increase in basal growth rates in the Autumn. The increase is particularly large in the NCEP simulation where congelation growth increases by 74% on average over the October, November and December~~, partially compensating the large increase in melting~~. The average increase in basal growth rates in the HadGEM2-ES forced simulation is ~~a more modest~~ much lower at 17%. ~~Note here we use $2.5\times10^{-3}\mathrm{m}^3\mathrm{m}^{-2}\mathrm{day}^{-1}$ as the threshold for melting starting and ending to capture the main phases of melt and growth.~~

In the *becomes MIZ* region the increase in peak rate of melting is again larger in the NCEP simulation, but not as dramatic as in the *always pack* region. Peak total melting rates increase by 29% in the NCEP and 13% in the HadGEM2-ES forced simulation and there is a shift in the melting season in the 2010s relative to the 1980s. The start of melting shifts earlier by 9 days in the NCEP and 5 days in the HadGEM2-ES forced simulation, whilst the end of summer melting ends later by 16 days later in the NCEP and 14 days in the HadGEM2-ES forced simulation, lengthening the melt season. Peak melting occurs

much earlier by 20 days in the NCEP and 12 days in the HadGEM2-ES forced simulation. The change in growth over October, November and December where the growth rates are typically increasing ~~contrast~~ differs between the two simulations~~. In the NCEP simulation there is a 17% increase, whilst in the HadGEM2-ES simulation there is a 6% decrease, likely due to the larger melt rates~~ , with a larger increase in the NCEP simulation.

In the *always MIZ* region the melt peaks stays a similar magnitude and occurs at a similar time, only a few days earlier in both simulations. Melting onset shifts slightly earlier by 6 days in the NCEP and 5 days in the HadGEM2-ES simulation. In the HadGEM2-ES simulation there is a significant shift earlier in the end of melting by 19 days (just 4 days earlier in the NCEP simulation), reflecting a significant reduction in summer ice in that region in the simulation. Growth rates in both simulations decrease over the October-December period, with the NCEP average decreasing by 16% and the HadGEM2-ES average decreasing by 20%.

In the projection, moving from the 2010s to the 2040s we see the same trends in the *becomes MIZ* and *always MIZ* regions as seen in the 1980s to 2010s comparison. The start of melting shifts earlier by 7 days in both the *becomes MIZ* and *always MIZ region*. The melt season shrinks, mostly due to the large shift on the end of the melt season, by 20 days in the *becomes MIZ* region and 21 days in the *always MIZ* region. This reflects all of the ice in those regions having melted. This is combined with a later start to congelation growth in the Autumn by 9 days in the *becomes MIZ* region and 21 days in the *always MIZ* region, followed by slower growth rates in both regions, 17% and 37% slower in the *becomes MIZ* and *always MIZ* regions over October, November and December.

4 Discussion

Our use of a forced atmosphere model does have potential implications for the results and their interpretation. The lack of a coupled atmosphere means there might be missing feedbacks, though it is possible this impact is not as large as previously assumed (Kay et al., 2016). Note that using coupled and climate models introduces its own set of problems, e.g. CMIP6 models fail to simulate a realistic seasonal cycle of sea ice area (Notz and Community., 2020). Using a forced sea ice model allows us to simulate a more realistic sea ice state, which has been shown to affect the balance of sea ice processes (Holland et al., 2010; Keen et al., 202
We chose to run simulations with the NCEP and HadGEM2-ES forcing so that the NCEP forced simulation could act as a check on the HadGEM2-ES forced simulation, which is projected to 2050. The two simulations were relatively similar in terms of sea ice extent, MIZ extent (see Section 2.2) and MIZ fraction (see Figure 7). Largely the overall results and proportions of growth and melt were similar in the two simulations, however the changes between the 1980s to the 2010s were generally larger in the NCEP forced simulation. This includes the changes in volume fluxes in both regions (see Figures 8a-f), reflecting the larger reduction in summer sea ice volume between the two periods (see Figure 5a). The differences between the NCEP and HadGEM2-ES forced simulations volume changes are largely a reflection of HadGEM2-ES having a much lower sea ice volume in the 1980s, however as the simulations become closer over time, it is difficult to assess whether the HadGEM2-ES simulation is underestimating the change from the 2010s to the 2040s.

~~Regions of the Arctic sea ice cover defined from daily July ice concentration fields from each time period from the NCEP and HadGEM2-ES forced simulations. Region 1 (blue) indicates the area that is pack ice in both the 1980s(2010s) and 2010s(2040s) in subplots a-d(e). Region 2 (green) indicates the area that is pack ice in the 1980s(2010s) and becomes MIZ in the 2010s(2040s) in subplots a-d(e). Region 3 (orange) indicates the area that is MIZ in both the 1980s(2010s) and the 2010(2040s) in subplots a-d(e).~~

~~14% 20% 19% 42% 46% 50% 30% 59% - 93% - -~~

~~Table of July MIZ fractions for each time period, where MIZ fraction is the fraction of the sea ice extent which is defined as MIZ.~~

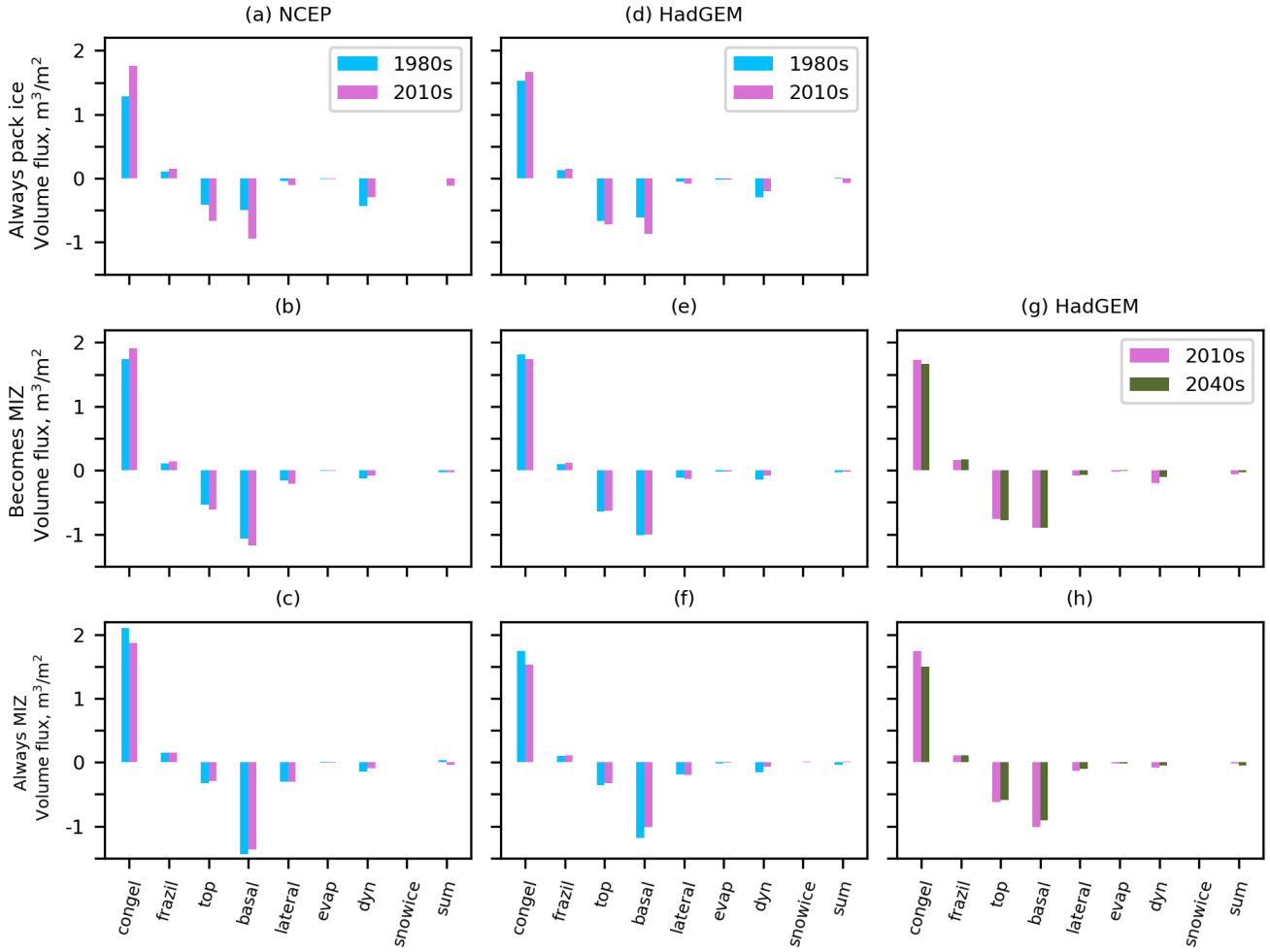

Figure 8. The total annual volume fluxes of sea ice in each of the regions shown in figure 6 for congelation ice growth, frazil ice formation, top melt, basal melt, lateral melt, sublimation, dynamics (transport, convergence and ridging), snow ice formation and the sum of all the terms. The summed annual volume fluxes are calculated from the average annual cycle in each time period. ~~A is the ice area, which is given for each time period and each region and is the annual average value.~~

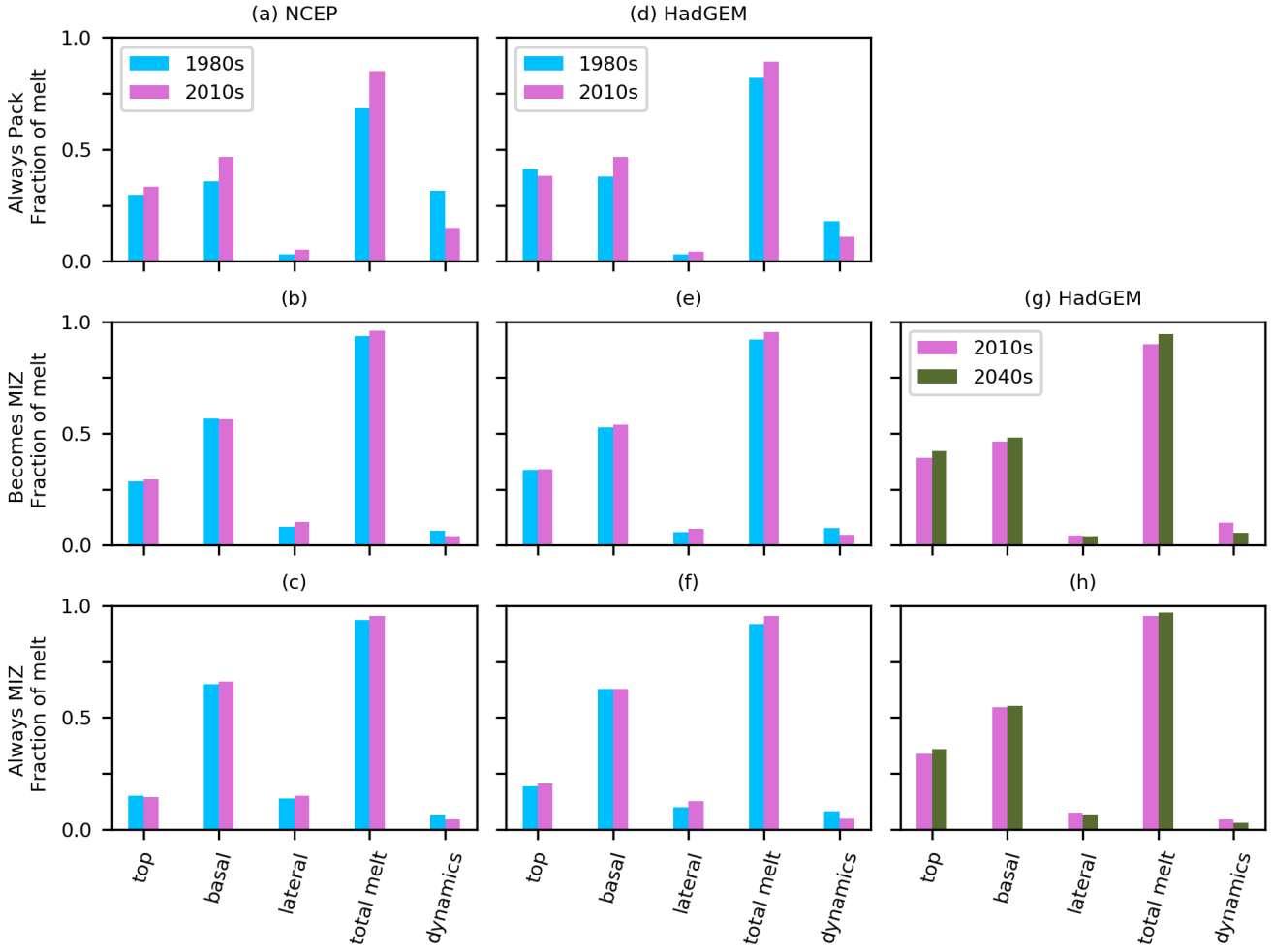

Figure 9. Fraction of ~~melt~~ ice loss that is top, basal and lateral ~~in each region and time period~~melt compared dynamics. The total for ice loss used does not include evaporation.

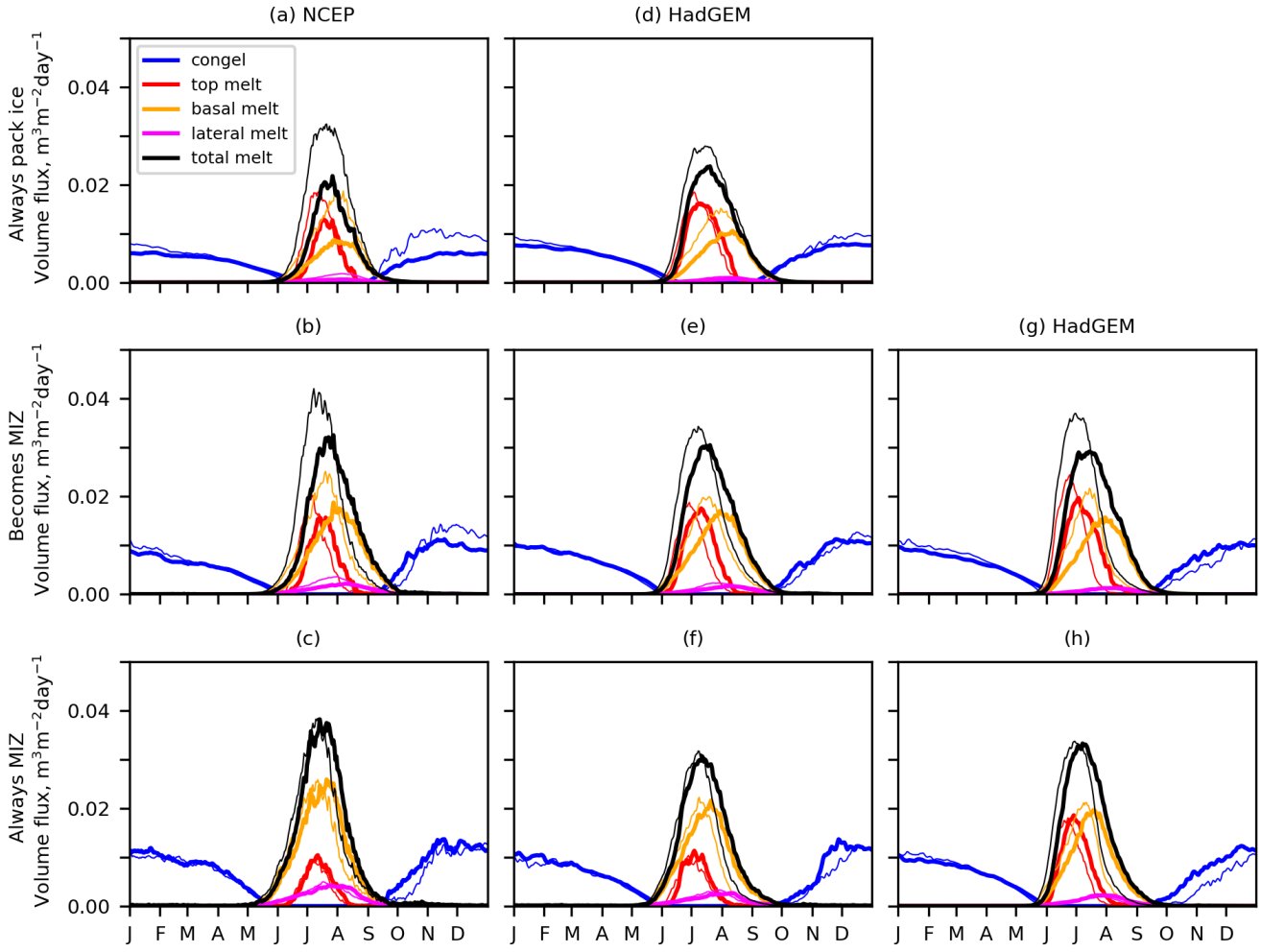

Figure 10. The time averaged annual cycles of congelation ice growth, top melt, basal melt and lateral melt in the regions described in Figure 6. The ~~solid line~~ thick lines show the 1980s average in subplots (a-f) and the 2010s in subplots (g-h). The ~~dashed~~ thin lines show the 2010s average in the subplots (a-f) and the 2040s in subplots (g-h).

Our forced sea ice-mixed layer model receives no trend in subsurface ocean properties, such as the "Atlantification" of the Arctic as the subsurface Atlantic Water layer becomes warmer and thicker (Grabon et al., 2021), which has the potential to cause sea ice loss if the heat reaches the surface (Polyakov et al., 2013; Onarheim et al., 2014; Carmack et al., 2015). It is possible that some of the relative increase in top melting could be due to the constant ocean forcing, which may lack some ocean warming that we might expect to see in the 2040s. Although how much of this heat is mixed into the upper layer that interacts with the sea ice is an open question. Additionally, field observations indicate that the majority of the ocean heat needed to explain basal ice melt rates can be explained from solar radiation (Perovich et al., 2011), something our model does capture.

The CICE model set up we used is relatively physics rich, which we believe is needed to represent the contrast between the pack ice and MIZ, as well as some of the changes over time. The differences in lateral melting was very likely caused by the inclusion of the FSTD model (Roach et al., 2018, 2019; Bateson et al., 2022), although we did not directly test this within this study. It is possible that lateral melt might be increased by the inclusion of a full wave model, though Bateson et al. (2022) show brittle fracture is likely just as important, and more so in the pack ice. The increase in top melting in the 2040s in the projection supports the importance of the topological melt pond scheme (Flocco et al., 2010, 2012) that we use, and the increasing role that melt ponds play in the sea ice mass balance and evolution. As an increasing fraction of the summer sea ice cover becomes MIZ we expect that the representation of FSD-wave interactions and the melt processes themselves is likely crucial to realistically representing Arctic sea ice and the transition to sea ice free summers. The representation, or lack of representation, of such processes can contribute to discrepancies of Arctic sea ice (Diamond et al., 2021).

Our results show that sea ice volume fluxes do have a dependence on ice concentration, as would be expected, supporting the separation of the sea ice cover into MIZ and non-MIZ regions for analysis of the volume budget. Our results also indicate that if we separated the MIZ (and the pack ice) into more ice concentration based categories we would see distinct behaviour in the balances of processes, particularly in the type of melting. The MIZ and pack ice divide we have used differentiates between where internal stresses becomes important (SIC>80%), and where they become small in the MIZ, and the sea ice is in free drift. Our approach also has the advantage of simplicity, the more concentration categories the MIZ is split into, the more complex the analysis becomes, and the less clear the results. We believe we have struck a balance between the complexity required and keeping the analysis as simple as possible to understand. Although the ice is more dynamic in the MIZ, it was shown in this study to be a decreasing sea ice sink term due to the reduction in sea ice volume, meaning there is less sea ice to transport. Additionally, there was a relative increase in the melt terms, see Figure 8.

5 Concluding remarks

In this study we used a high physical fidelity sea ice model (CPOM version of CICE) coupled to a mixed layer model to compare the ice volume budget in the pack ice and the marginal ice zone (MIZ). To our knowledge, this is the first analysis of volume budget that explicitly segments between the pack ice and MIZ. The MIZ is defined as having ~~an~~ a sea ice concentration (~~A~~SIC) between 15% and 80% and pack ice is defined as ~~A~~SIC>80%. We ran two simulations, where the model is forced with

NCEP reanalysis (1980-2020) and HadGEM2-ES (1980-2050) atmospheric fields. We simulate a MIZ extent within the bounds of observational estimates from Bootstrap and NASA Team, giving us confidence that the model is simulating a realistic sea ice and MIZ state. The NCEP and HadGEM2-ES forced simulations give realistic (and similar) sea ice states over the historical period.

The 1980s *low MIZ* state, and the 2010s *high MIZ* state were compared in simulations using ~~by~~ NCEP and HadGEM2-ES forcing, and the 2010s *high MIZ* state was compared to the 2040s *all MIZ* state. The percentage of the summer sea ice cover that was MIZ increased from 14% in the 1980s to 46% in the 2010s in the NCEP forced simulation, and from 20% in the 1980s to 50% in the 2010s and 93% in the 2040s in the HadGEM2-ES forced simulation.

Sea ice growth was dominated by congelation growth across the pack ice and MIZ regions in all time periods/MIZ states studied, making up between 91-95%. Frazil made up 5-9% of sea ice growth whilst snow ice growth accounted for less than 1% of sea ice growth. There was no significant difference over time or between the pack ice and MIZ in the processes of sea ice growth. Dynamics acted as a volume sink in all regions, as sea ice is transported from the central Arctic to lower latitudes where it melts. Due to the decreasing sea ice volume this sea ice sink decreased over time in both simulations.

There was a significant contrast in the relative balance of basal, top and lateral melt in the pack ice and MIZ in the 1980s and 2010s in both simulations. Basal melting accounts for the largest portion of melting ~~making up 46-60% in regions of~~ in pack ice and ~~increasing slightly in regions of MIZ to 52-69%~~MIZ regions. Top melt was the next biggest melt term and was twice as important in ~~the region that was always pack ice compared to the region that was MIZ~~ pack ice regions compared to MIZ regions in both the 1980s and 2010s~~, making up 39-50% of melt in the regions that remained pack ice and 15-21% in the regions that remained MIZ~~. The opposite is true for lateral melting which ~~makes up 4-5%~~ made up twice as much of melting in the ~~region that remained pack ice~~MIZ relative to the pack ice, becoming comparable to top melting in MIZ defined region in the 1980s and ~~10-15% in regions that remained MIZ . However, in the projection into the~~ 2010s. There was little change in this between the 1980s and 2010s. However in the 2040s~~top melt formed an increased proportion of melting including in the MIZ, which forms most of the sea ice cover during this time period, with values of around 40%~~, there was an increase in top melting in all regions due to increasing surface air temperatures.

The timing of the annual seasonal cycles of growth and melt changed significantly in all regions. In the regions ~~that remains pack icein~~ of pack ice, from the 1980s and 2010s the total melting and growth rates increase, this is more pronounced in the NCEP forced simulation where we see an increase of 49% in the peak total melting rates which is partially compensated by an 74% increase in the average October-December growth rates. In the regions ~~that became or remained MIZ~~of MIZ, from the 1980s to the 2010s, and for the 2010s and 2040s, we see the melt season shift earlier. Additionally the end of summer melting shifts earlier in all of the regions, particularly in the region that is remains MIZ. This reflects that as the sea ice volume decreases we get to a point where all of the ice in these regions is melting over the summer, and a period in late summer starts to open up in these regions where there is no sea ice present.

Our analysis demonstrates a different balance of processes control the volume budget of the MIZ versus the pack ice. They are understandable in terms of the physical processes that are dependent on the ice concentration, such as wave-ice interaction and lateral melt, which we are able to account for in our relatively physics rich sea ice model. We suggest that representation

of such processes, in models such as climate models, requires more attention as a greater fraction of the sea ice cover becomes MIZ.

Author contributions. RF carried out the calculations and led the writing of the manuscript. DF and DS gave supervision. AB gave advice on the CICE set up and provided the local CICE version that was used. All authors were involved in the design and analysis of numerical simulations.

Competing interests. DF and DS are editors for The Cryosphere.

References

References

Aksenov, Y., Popova, E. E., Yool, A., Nurser, A. J. G., Williams, T. D., Bertino, L., , and Bergh, J.: On the future navigability of Arctic sea routes: High-resolution projections of the Arctic Ocean and sea ice, Mar. Pol., 75, 300–317, https://doi.org/10.1016/j.marpol.2015.12.027, 2017.

Bateson, A. W.: Fragmentation and melting of the seasonal sea ice cover, Ph.D. thesis, Department of Meteorology, University of Reading, United Kingdom, https://doi.org/10.48683/1926.00098821, 2021.

Bateson, A. W., Feltham, D. L., Schröder, D., Hosekova, L., Ridley, J. K., and Aksenov, Y.: Impact of sea ice floe size distribution on seasonal fragmentation and melt of Arctic sea ice, The Cryosphere, 14, 403–428, https://doi.org/10.5194/tc-14-403-2020, 2020.

Bateson, A. W., Feltham, D. L., Schröder, D., Wang, Y., Hwang, B., Ridley, J. K., and Aksenov, Y.: Sea ice floe size: its impact on pan-Arctic and local ice mass, and required model complexity, The Cryosphere, 16, 2565–2593, https://doi.org/10.5194/tc-16-2565-2022, 2022.

Bitz, C. M. and Lipscomb, W. H.: An energy-conserving thermodynamic model of sea icel, J. Geophys. Res.-Ocean., 104, 15 669–15 677, https://doi.org/10.1029/1999jc900100, 1999.

Briegleb, P. and Light, B.: A Delta-Eddington multiple scattering parameterization for solar radiation in the sea ice component of the Community Climate System Model, NCAR Technical Note TN-472+ STR, p. 100 pp, https://doi.org/10.5065/D6B27S71, 2007.

Carmack, E. C., Polyakov, I., Padman, L., Fer, I., Hunke, E., Hutchings, J., Jackson, J., Kelley, D., Kwok, R., Layton, C., Melling, H., Perovich, D., Persson, O., Ruddick, B., Timmermans, M.-L., Toole, J., Ross, T., Vavrus, S., and Winsor, P.: Toward quantifying the increasing role of oceanic heat in sea ice loss in the new Arctic, Bull. Am. Meteorol. Soc., 96), 2079–2105, https://doi.org/10.1175/BAMS-D-13-00177.1, 2015.

Cavalieri, D. J., Parkinson, C. L., Gloersen, P., and Zwally, H. J.: Sea Ice Concentrations from Nimbus-7 SMMR and DMSP SSM/I-SSMIS Passive Microwave Data, Version 1, Natl. Snow and Ice Data Cent., Boulder, CO [1980-2022], (last access: 31 December 2016), https://doi.org/http://nsidc.org/data/NSIDC-0051/versions/1.html, 1996.

Comiso, J. C.: Bootstrap Sea Ice Concentrations from Nimbus7 SMMR and DMSP SSM/I-SSMISVersion 3, NASA National Snow and Ice Data Center Distributed Active Archive Center, Boulder, Colorado USA [1980-2022], https://doi.org/10.5067/7Q8HCCWS4I0R, 2017.

Dee, D. P., Uppala, S. M., Simmons, A. J., Berrisford, P., Poli, P., Kobayashi, S., Andrae, U., Balmaseda, M. A., Balsamo, G., Bauer, P., Bechtold, P., Beljaars, A. C. M., van de Berg, L., Bidlot, J., Bormann, N., Delsol, C., Dragani, R., Fuentes, M., Geer, A. J., Haimberger, L., Healy, S. B., Hersbach, H., Hólm, E. V., Isaksen, L., Kållberg, P., Köhler, M., Matricardi, M., Mcnally, A. P., Monge-Sanz, B. M., Morcrette, J. J., Park, B. K., Peubey, C., de Rosnay, P., Tavolato, C., Thépaut, J. N., and Vitart, F.: The ERA-Interim reanalysis: Configuration and performance of the data assimilation system, Q. J. Roy. Meteor. Soc., 137), 553–597, https://doi.org/10.1002/qj.828, 2011.

Diamond, R., Sime, L. C., Schroeder, D., and Guarino, M. V.: The contribution of melt ponds to enhanced Arctic sea-ice melt during the Last Interglacial, The Cryosphere, 15), 5099–5114, https://doi.org/10.5194/tc-15-5099-2021, 2021.

Dumont, D., Kohout, A., and Bertino, L.: A wave-based model for the marginal ice zone including a floe breaking parameterization, J. Geophys. Res.-Ocean., 116), C04 001, https://doi.org/10.1029/2010JC006682, 2011.

Ferry, N., Masina, S., Storto, A., Haines, K., and Valdivieso, M.: Product User Manual GLOBALREANALYSISPHYS-001-004- a and b, MyOcean, 2011.

Flocco, D., Feltham, D. L., and Turner, A. K.: Incorporation of a physically based melt pond scheme into the sea ice component of a climate model, J. Geophys. Res.-Ocean., 115, C08 012, https://doi.org/10.1029/2009JC005568, 2010.

Flocco, D., Schroeder, D., Feltham, D. L., and Hunke, E. C.: Impact of melt ponds on Arctic sea ice simulations from 1990 to 2007, J. Geophys. Res.-Ocean., 117, C09 032, https://doi.org/10.1029/2012JC008195, 2012.

Grabon, J. S., Toole, J. M., Nguyen, A. T., and Krishfield, R. A.: An analysis of Atlantic water in the Arctic Ocean using the Arctic subpolar gyre state estimate and observations, Progress in Oceanography, 198, 102 685, https://doi.org/10.1016/j.pocean.2021.102685, 2021.

Heorton, H. D. B. S., Feltham, D. L., and Tsamados, M.: Stress and deformation characteristics of sea ice in a high-resolution, anisotropic sea ice model, Philos. Trans. R. Soc. A, 376, 20170 349, https://doi.org/10.1098/rsta.2017.0349, 2018.

Hibler, W. D.: A Dynamic Thermodynamic Sea Ice Model, J. Phys. Ocean., 9(4), 815–846, https://doi.org/10.1175/1520-0485(1979)009<0815:ADTSIM>2.0.CO;2, 1979.

Holland, M. M., Serreze, M. C., , and Stroeve, J.: The sea ice mass budget of the Arctic and its future change as simulated by coupled climate models, Clim. Dynam., 34, 185–200, https://doi.org/10.1007/s00382-008-0493-4, 2010.

Holland, P. and Kimura, N.: Observed concentration budgets of Arctic and Antarctic sea ice, J. Clim., 29, 5241–5249, https://doi.org/10.1175/JCLI-D-16-0121, 2016.

Horvat, C., Blanchard-Wrigglesworth, E., and Petty, A. A.: Observing waves in sea ice with ICESat-2, Geophys. Res. Lett., 47, e2020GL087 629, https://doi.org/10.1029/2020GL087629, 2020.

Hunke, E. C., Lipscomb, W. H., Turner, A. K., Jeffery, N., and Elliott, S.: CICE: the Los Alamos Sea Ice Model Documentation and Software User's Manual Version 5.1, 2015.

Jones, C. D., Hughes, J. K., Bellouin, N., Hardiman, S. C., Jones, G. S., Knight, J., Liddicoat, S., O'Connor, F. M., Andres, R. J., Bell, C., Boo, K. O., Bozzo, A., Butchart, N., Cadule, P., Corbin, K. D., Doutriaux-Boucher, M., Friedlingstein, P., Gornall, J., Gray, L., Halloran, P. R., Hurtt, G., Ingram, W. J., Lamarque, J. F., Law, R. M., Meinshausen, M., Osprey, S., Palin, E. J., Parsons Chini, L., Raddatz, T., Sanderson, M. G., Sellar, A. A., Schurer, A., Valdes, P., Wood, N., Woodward, S., Yoshioka, M., and Zerroukat, M.: The HadGEM2-ES implementation of CMIP5 centennial simulations, Geosci. Model Dev.,, 4, 543–570, https://doi.org/10.5194/gmd-4-543-2011, 2011.

Kanamitsu, M., Ebisuzaki, W., Woollen, J., Yang, S.-K., Hnilo, J. J., Fiorino, M., and Potter, G. L.: NCEP–DOE AMIPII Reanalysis (R-2), B. Am. Meteorol. Soc., 83, 1731–1643, https://doi.org/10.1175/BAMS-83-11-1631, 2002, (updated 2017).

Kay, J. E., L'Ecuyer, T., Chepfer, H., Loeb, N., Morrison, A., and Cesana, G.: Recent Advances in Arctic Cloud and Climate Research, Curr Clim Change Rep, 2, 159–169, https://doi.org/10.1007/s40641-016-0051-9, 2016.

Keen, A. and Blockley, E.: Investigating future changes in the volume budget of the Arctic sea ice in a coupled climate model, The Cryosphere, 12, 2855–2868, https://doi.org/10.5194/tc-15-951-2021, 2018.

Keen, A., Bailey, D., Debernard, J. B., Bushuk, M., Delhaye, S., Docquier, D., Feltham, D., Massonnet, F., O'Farrell, S., Ponsoni, L., é M. Rodriguez, J. M., Schröeder, D., Swart, N., Toyoda, T., Tsujin, H., Vancoppenolle, M., and Wyser, K.: An inter-comparison of the mass budget of the Arctic sea ice in CMIP6 models, The Cryosphere, 15, 951–982, https://doi.org/10.5194/tc-15-951-2021, 2021.

Lipscomb, W. H. and Hunke, E. C.: Modeling Sea Ice Transport Using Incremental Remapping, Mon. Weather Rev., 132, 1341–1354, https://doi.org/10.1175/1520-0493(2004)132<1341:msitui>2.0.co;2, 2004.

Martin, T., Tsamados, M., Schroeder, D., and Feltham, D.: The impact of variable sea ice roughness on changes in Arctic Ocean surface stress: A model study, J. Geophys. Res. Oceans, 121, 1931–1952, https://doi.org/10.1002/2015JC011186, 2016.

Maykut, G. A. and Untersteiner, N.: Some results from a timedependent thermodynamic model of sea ice, J. Geophys. Res., 76, 1550–1575, https://doi.org/10.1029/jc076i006p01550, 1971.

Notz, D. and Community., S.: Arctic sea ice in CMIP6, Geophys. Res. Lett., 47, e2019GL086 749, https://doi.org/10.1029/2019GL086749, 2020.

Notz, D., Jahn, A., Holland, M., Hunke, E., Massonnet, F., Stroeve, J., Tremblay, B., and Vancoppenolle, M.: The CMIP6 Sea-Ice Model Intercomparison Project (SIMIP): understanding sea ice through climate-model simulations, Geosci. Model Dev., 9, 3427–3446, https://doi.org/10.5194/gmd-9-3427-2016, 2016.

Onarheim, I. H., Smedsrud, L. H., Ingvaldsen, R., and Nilsen, F.: Loss of sea ice during winter north of Svalbards, Tellus, 668, 23 933, https://doi.org/10.3402/tellusa.v66.23933, 2014.

Perovich, D K. Richter-Menge, J. A., Jones, K. F., Light, B., Elder, B. C., Polashenski, C., Laroche, D., Markus, T., and Lindsay, R.: Arctic sea-ice melt in 2008 and the role of solar heating, Ann. Glaciol., 52, 355–359, https://doi.org/10.3189/172756411795931714, 2011.

Petty, A. A., Holland, P. R., and Feltham, D. L.: Sea ice and the ocean mixed layer over the Antarctic shelf seas, The Cryosphere, 8, 761–783, https://doi.org/10.5194/tc-8-761-2014, 2014.

Polyakov, I. V., Pnyushkov, A. V., Rember, R., Padman, L., Carmack, E. C., and Jackson, J. M.: Winter convection transports Atlantic water heat to the surface layer in the eastern Arctic Ocean, J. Phys. Ocean., 43, 2142–2155, https://doi.org/10.1175/JPO-D-12-0169.1, 2013.

Roach, L. A., Dean, S. M., and Renwick, J. A.: Consistent biases in Antarctic sea ice concentration simulated by climate models., The Cryosphere, 12(1), 365–383, https://doi.org/10.5194/tc-12-365-2018, 2018.

Roach, L. A., Bitz, C. M., Horvat, C., and Dean, S. M.: Advances in modeling interactions between sea ice and ocean surface waves, J. Adv. Model. Earth Syst., 11, 4167–4181, https://doi.org/10.1029/2019MS001836, 2019.

Rolph, R. J., Feltham, D. L., and Schröder, D.: Changes of the Arctic marginal ice zone during the satellite era., The Cryosphere, 14, 1971–1984, https://doi.org/10.5194/tc-14-1971-2020, 2020.

Rothrock, D. A.: The energetics of the plastic deformation of pack ice by ridging, J. Geophys. Res., 80, 4514–4519, https://doi.org/10.1029/jc080i033p04514, 1975.

Schröder, D., Feltham, D. L., Tsamados, M., and Ridout, A.: New insight from CryoSat-2 sea ice thickness for sea ice modelling, The Cryosphere, 13, 125–139, https://doi.org/10.5194/tc-13-125-2019, 2019.

Strong, C. and Rigor, I. G.: Arctic marginal ice zone trending wider in summer and narrower in winter, Geophys. Res. Lett., 40, 4864–4868, https://doi.org/10.1002/grl.50928, 2013.

Tsamados, M., Feltham, D. L., Schröder, D., Flocco, D., Farrell, S. L., Kurtz, N., Laxon, S. W., and Bacon, S.: Impact of Variable Atmospheric and Oceanic Form Drag on Simulations of Arctic Sea Ice*, J. Phys. Ocean., 44(5), 4864–4868, https://doi.org/10.1175/JPO-D-13-0215.1, 2014.

Wang, M. and Overland, J. E.: A sea ice free summer Arctic within 30 years: An update from CMIP5 models, Geophys. Res. Lett., 39, L18 501, https://doi.org/10.1029/2012GL052868, 2012.

Wilchinsky, A. V. and Feltham, D. L.: Modelling the rheology of sea ice as a collection of diamond-shaped floes, J. Nonnewton. Fluid Mech., 138, 22–32, https://doi.org/10.1016/j.jnnfm.2006.05.001, 2006.

Zhang, J. L. and Rothrock, D. A.: Modelling global sea ice with a thickness and enthalpy distribution model in generalized curvilinear coordinates, Mon. Weather Rev., 131, 845–861, https://doi.org/10.1175/1520-0493(2003)131<0845:MGSIWA>2.0.CO;2, 2003.